

Leveraging a Necroptosis Pattern to Predict the Prognosis and Drug Sensitivity of Ovarian Cancer

Chang-Zhong Li*, Na Su, Ping-Ping Cai, Xiao-Xue Yin, Hong-Min Xu, Zhi-Qiang Dou

Department of Medical Science, Shandong University of Traditional Chinese Medicine, Jinan, China

Research Article

Received: 25-May-2023, Manuscript No. JPPS-23-99950; **Editor assigned:** 29-May-2023, Pre QC No. JPPS-23-99950 (PQ); **Reviewed:** 12-Jun-2023, QC No. JPPS-23-99950; **Revised:** 25-Aug-2023, Manuscript No. JPPS-23-99950 (R); **Published:** 01-Sep-2023, DOI: 10.4172/2320-1215.12.4.007

***For Correspondence:** Zhong Li, Department of Medicinal Science, Shandong University of Traditional Chinese Medicine, Jinan, China; **Email:** lichangzhong_sd@sina.com

Citation: Zhong CLi, et al. Leveraging a Necroptosis Pattern to Predict the Prognosis and Drug Sensitivity of Ovarian Cancer. RRJ Pharm Pharm Sci. 2023;12:007.

Copyright: © 2023 Zhong CLi, et al. This is an open-access article distributed under the terms of the Creative Commons Attribution License, which permits unrestricted use, distribution and reproduction in any medium, provided the original author and source are credited.

ABSTRACT

Background: Ovarian Cancer (OC) remains a fatal gynecological malignancy. Necroptosis may be a backup pathway that induces cell death when apoptosis is inhibited. This research aims to develop and validate an OC prognosis model based on necroptosis.

Methods: The Cancer Genome Atlas (TCGA) and Genome Tissue Expression Consortium Project Genome (GTEx) databases were used in obtaining data on OC patients and normal ovarian tissues. Necroptosis related genes were downloaded from the Kyoto Encyclopedia of Genes and Genomes (KEGG) database. Differentially Expressed Genes (DEGs) between tumors and normal tissues were screened. COX regression analysis was used in constructing gene signature, which was further tested and validated in the TCGA and GEO cohorts. Based on risk scores and different clinical prognostic features, Nomogram was constructed to predict OS in OC patients. Then, the patients were divided into high- and low-risk groups, and differential genes were identified between the two groups. The potential biological and pathological functions of the differential genes were explored through Gene Ontology (GO) and KEGG analyses. Immunoassays were used to analyze immune status. Immunohistochemistry (IHC) further confirmed the expression levels of core prognostic genes and their correlations with Overall Survival (OS) rates. Drug sensitivity analysis in different risk groups was performed to screen out potential drugs for the treatment of OC. Finally, a consensus clustering analysis was used in subtyping ovarian tumors.

Results: A three gene signature was identified, including JAK1, PYGB, and STAT1. The high-risk group had lower OS than the low-risk group and the risk score was acceptable for predicting prognosis independent of any other clinical prognostic features. The nomogram can accurately predict the 1, 3, and 5 year survival rates of patients with OC. Functional analysis revealed immune related pathways and differences in immune status between the two risk groups. Furthermore, three core prognostic genes involved in model construction were overexpressed in OC

versus those in normal ovarian tissues. Patients in the low-risk group were more sensitive to cisplatin and docetaxel. In consensus clustering analysis, OC patients were separated into two subtypes and the survival rate in cluster 1 was better than in cluster 2.

Conclusion: A necroptosis related model based on three cores prognostic DEGs can be used to predict OC prognosis.

Keywords: Ovarian cancer; Prognostic signature; Necroptosis; Cell death; Overall survival

INTRODUCTION

Ovarian Cancer (OC) is one of the most lethal gynecologic malignancies worldwide. It is often detected at a late stage because of the lack of specific clinical symptoms in the early stages and patients with OC have a 5 year survival rate of approximately 30%–50%. Unfortunately, curative treatments for women with recurrent OC are currently unavailable. Given the poor prognoses and low survival rates of patients with OC, finding early detection modes that can aid the diagnosis and prognosis of OC, including clinical biomarkers or prognostic models, remains a considerable challenge. CA125 has been accepted as a serum biomarker protein and approved for OC monitoring, but it only has a sensitivity of approximately 40% and poorly predicts early stage patients. Nevertheless, an accurate prognostic model based on different clinicopathologic variables may serve as a crucial tool for aiding clinical decisions. Therefore, developing a prognostic model for OC is particularly important [1].

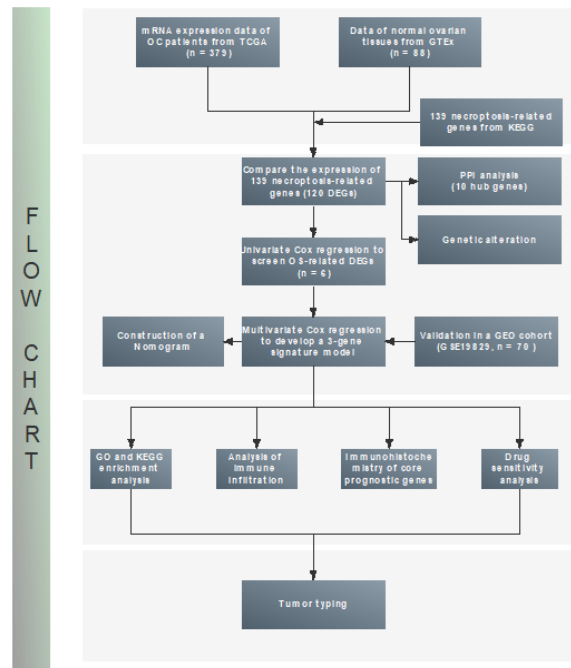
Apoptosis is a conserved fundamental biological cell death process. Effective cancer therapy largely depends on the induction of apoptosis that kills cancer cells through chemotherapy and radiation. The evasion of apoptosis is a common mechanism that contributes to drug resistance and tumour progression. To a large extent, apoptosis resistance is a major obstacle leading to the failure of cancer treatments. Thus, inducing cancer cell death bypassing the apoptotic pathway is challenging. Necroptosis may serve as a backup pathway that enables cell death when apoptosis is inhibited and cancer cells resistant to apoptosis may be sensitive to necroptosis. Hence, necroptosis may be a solution. More specifically, the pertinence of necroptosis and cancer are promising novel targets in cancer diagnosis and treatment [2].

However, the relationship between necroptosis and the prognosis of OC is complex and incompletely understood. Over the past few years, many clinical prognostic models associated with cell death, including autophagy models and gene signature and ferroptosis related models, have been developed to predict the risk of OC. By contrast, necroptosis related models have never been studied. To further explore the association between necroptosis and OS of patients with OC, we aimed to develop and externally validate a necroptosis related prognostic model [3].

In our study, we first collected data pertinent to patients with OC and normal human ovarian tissues from public databases and then identified Differentially Expressed Genes (DEGs) associated with necroptosis. Furthermore, we further screened genes related to the OS of patients with OC in the TCGA database and established a necroptosis related model for OC prognosis. This model was subsequently tested in the Gene Expression Omnibus (GEO) cohort utilizing multiple data analysis methods. Finally, we performed enrichment analysis and analysis of immune correlates and constructed a Nomogram model. IHC further confirmed the expression levels of core prognostic genes and their correlations with OS. To screen out potential drugs for the treatment of OC, we further analyzed and predicted the differences in the sensitivity of different

chemotherapy drugs in high and low risk groups. Finally, a consensus clustering analysis was used in subtyping ovarian tumors. The general overview of the steps is depicted in Figure 1.

Figure 1. The flow chart of this study.



MATERIALS AND METHODS

Data collection

To develop a necroptosis related prognosis model for OC, we downloaded the datasets of 379 patients with OC. RNAseq data and clinically relevant information were obtained from the TCGA database, and 88 normal human ovarian tissue samples were obtained from the GTEx database. In the external validation cohort, information was collected from the GEO database, and 70 samples from GSE19829 were used in verifying this model. All data in our study are publicly available, and thus using them causes no ethical concern [4].

Identification of necroptosis related DEGs

Based on KEGG database, 139 necroptosis related genes were downloaded. Differential necroptosis expression genes were then compared and identified from OC and normal human ovarian tissues by using the “limma” R package, and a P-value of <0.05 indicated a significant difference. The DEGs were visualized with a heat map and notated as follows: * if P<0.05, ** if P<0.01, and *** if P<0.001.

Moreover, we identified the Protein–Protein Interaction (PPI) network to explore the interactions of the necroptosis related genes, using the string database within the limits of the interaction threshold (0.7). However, the network was highly disarrayed because of the large number of genes. Thus, 10 genes were screened as hub genes and further decorated using

cytoscape software [5]. To explore the clinical value of the hub genes, we examined their genetic alterations (gene mutations and copy number variations) with cBioPortal for cancer genomics [6].

Establishment and validation of a necroptosis related gene prognosis model

To further assess the prognostic values of the necroptosis related genes, DEGs closely related to OS were screened through univariate regression analysis, and the significance criterion was set (adjusted $P < 0.05$). Then, candidate prognostic genes were screened through multivariate regression analysis, and a novel prognostic model was constructed.

Furthermore, our study developed a risk assessment model for each patient in the TCGA cohort according to gene expression level and regression coefficient, and the patients were divided into high- and low-risk groups according to the median risk score. The formula of risk score was as follows: Risk score = $0.445 \times$ expression level of *JAK1* + $0.093 \times$ expression level of *PYGB* + $(-0.381) \times$ expression level of *STAT1*. Subsequently, risk analyses were performed for the evaluation and testing of this model. The OS probability between high and low risk clusters was provided by the Kaplan–Meier (KM) curve. According to the “survival,” “survminer,” and “timeROC” R packages, Receiver Operating Characteristic curves (ROCs) were useful in assessing the diagnostic accuracy of the risk prediction model. The “pheatmap” package in R software was used in showing the survival status for each patient in the TCGA cohort. Dimension reduction algorithms for the gene signature model, including Principal Component Analysis (PCA) and t-Stochastic Neighbour Embedding (t-SNE), were implemented for the visualization of the expression of DEGs. “Rtsne” and “ggplot2” R packages were used. Finally, we used the risk scores and clinical traits, such as age and grade, of the OC samples to evaluate the independent prognostic value of the model in univariable and multivariate analyses [7].

Furthermore, we used GSE19829 from the GEO database as an external test cohort and carried out a series of risk analyses in the GEO cohort to validate the accuracy of the risk prediction model.

Nomogram establishment based on various prognostic indicators

Based on various prognostic indicators such as age, stage, race, and risk score, we constructed a nomogram prediction model to predict the 1, 3, and 5 year survival rates of OC patients. In the calibration chart, the predictive accuracy of the nomogram model is evaluated by comparing the actual probabilities and the model-predicted probabilities for different scenarios [8].

Expression of each gene involved in model construction in low and high risk groups

The OC cases were categorized into low and high risk groups on the basis of the median cut off value from the TCGA cohort. We drew a heat map to explain the expression of each gene involved in the model construction in the low and high risk groups and determine high and low risk genes. In addition, we further explored whether differences in the clinical traits of OC cases between the high and low risk groups [9].

Functional enrichment of necroptosis related degs

Necroptosis related genes differentially expressed in the high- and low-risk groups performed were identified according to a set threshold of the absolute value of $\text{Log}_2\text{FC} \geq 0.585$ and a False Discovery Rate (FDR) of < 0.05 . Subsequently, the DEGs identified were subjected to GO functional annotation and KEGG pathway enrichment analysis using the ClusterProfile and ggplot2 R package.

Immune infiltration

First, the ssGSEA algorithm was used in calculating the scores of infiltration immune cell types and immune-related functions in each sample. Then, the analysis was outlined as Box plot for the visualization of the different levels of infiltration of immune cell types and immune functions in the high- and low-risk groups from the OC expression profile of the TCGA database [10].

Identification of each gene involved in model construction in OC based on the human protein atlas database

By harnessing the Human Protein Atlas (HPA) database, we obtained the immunohistochemistry of each gene involved in model in normal human ovarian tissues and OC tissues.

Tumour typing based on the expression of necroptosis related degs

In the last step, consensus clustering analysis was used in subtyping human ovarian tumors from the TCGA database on the basis of the expression of necroptosis related DEGs. According to k, the most suitable number of clusters, patients with OC can be subdivided into various subtypes. Furthermore, we performed survival analysis to determine whether or not differences among the clusters of OC patients are significant.

Drug sensitivity analysis

To explore differences in drug sensitivity across risk groups, we calculated the IC50 of the drug using the pRRophetic R package.

Statistical analysis

All statistical analyses were performed with R (version 4.1.1; 2021-08-10). In the comprehensive analysis, a P value of <0.05 indicated statistical significance. Differential necroptosis gene expression between OC and normal human ovarian tissues was compared with Wilcox test and the “limma” R package. The OS of different groups was compared through KM analysis with log rank test. The Mann–Whitney test was used in comparing different levels of infiltration of immune cell types and immune related functions between the high and low risk groups [11].

Data availability statement

All data generated or analyzed during this study are included in this published article and its supplementary information files.

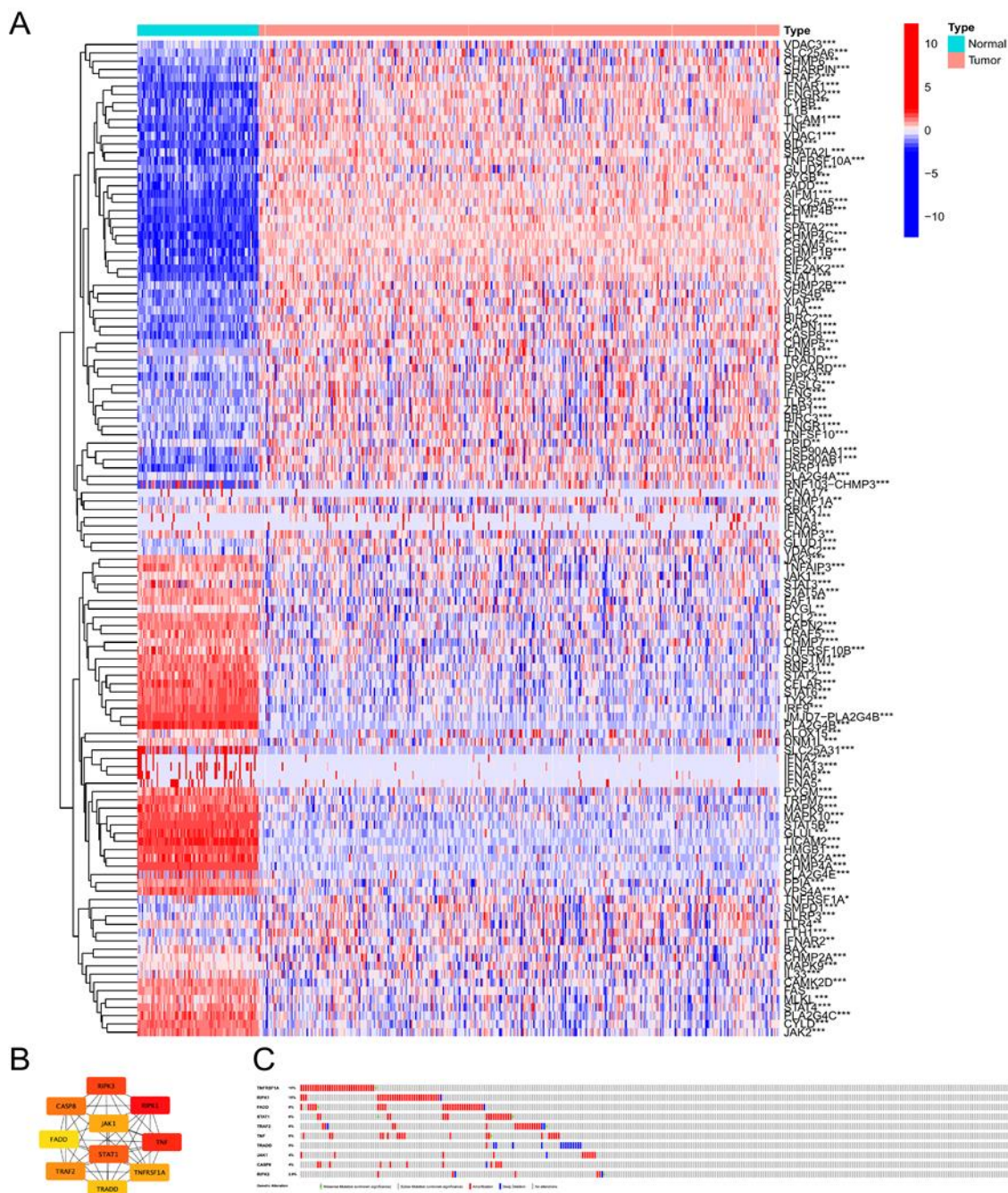
RESULTS

Necroptosis related DEGs in OC

A total of 379 patients with OC from the TCGA and 88 normal ovarian tissues from the GTEx were collected, and 139 necroptosis related genes were downloaded from the KEGG database. The expression of 133 necroptosis related genes was extracted from the expression matrix of the TCGA and GTEx transcriptome. Through differential gene expression analysis, we identified 120 necroptosis related DEGs detected in normal ovarian samples and OC samples and visualized them by using heatmaps. As shown in Figure 2A, some necroptosis genes were up-regulated in the OC cases, including VDAC3, TNF, and STAT1. Other genes were down regulated in the tumour samples, such as JAK1, PYG1, and BCL2.

In addition, the PPI network of 10 hub genes, namely, STAT1, JAK1, TNF, TNFRSF1A, TRADD, FADD, CASP8, TRAF2, RIPK1, and RIPK3, was shown in Figure 2B. As for the genetic alterations of 10 hub genes, we found that queried genes were altered in 127 (41%) queried samples, mainly including changes in deep deletion or amplification, and missense mutation was the major form of the gene mutations. Finally, 10 genes are shown in Figure 2C. TNFRSF1 and RIPK1 were the most frequently mutated genes, with the same genetic alteration rate of 10%.

Figure 2. (A) 120 necroptosis related DEGs of normal ovarian and OC samples; (B) The PPI network; and (C) Genetic alterations of 10 hub genes.

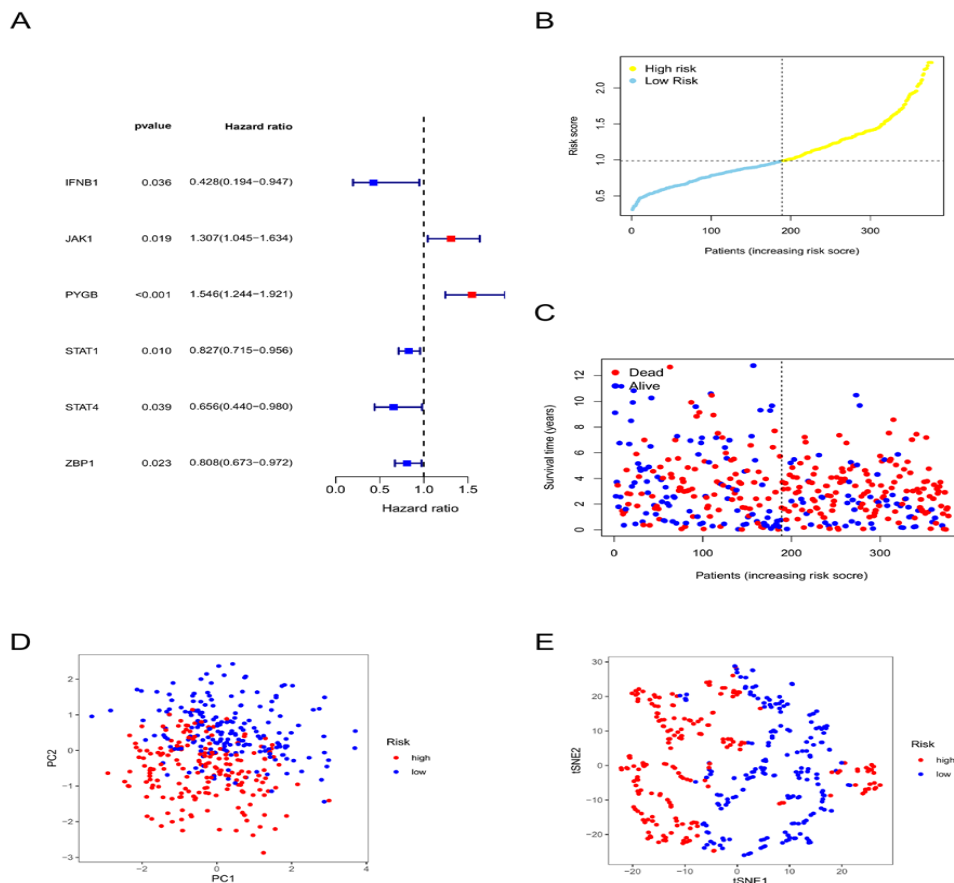


Construction of a prognostic risk model

Given the effect of differential genes on OS of patients with OC, univariate regression survival analysis was used in identifying necroptosis-related genes associated with prognosis. Six genes: *IFNB1*, *JAK1*, *PYGB*, *STAT1*, *STAT4*, and *ZBP1*, were finally screened. Notably, *IFNB1*, *STAT1*, *STAT4*, and *ZBP1* belonged to low-risk genes (Hazard Ratio (HR) <1, P<0.05), whereas *JAK1* and *PYGB* belonged to high-risk genes (HR>1, P<0.05), which are shown in Figure 3A (low risk genes were marked in blue, and high risk genes were marked in red). According to the expression of the six genes mentioned above, multivariate regression analysis was used in screening candidate prognostic genes. Eventually, three risk genes (*i.e.*, *JAK1*, *PYGB*, and *STAT1*) were used in constructing the model, and the risk scores for each patient were calculated using their gene expression levels and regression coefficients [12].

First, using the median risk score from the TCGA cohort as a benchmark, we divided the OC cases into high and low risk groups. As shown in a risk plot, the high risk group is shown in yellow, whereas the low-risk group is shown in sky blue (Figure 3B). Then, we profiled the survival status of each patient in the TCGA cohort. Patients who died were marked in red, and those who survived were marked in blue. The results showed that as the risk of patients increased with the number of deaths (Figure 3C). Subsequently, PCA and t-SNE analysis (Figure 3D and 3E) were used in dimension reduction for the visualization of the three genes involved in modelling in a two-dimensional space. Patients from different risk groups were separated in both directions. The genes above can be used in distinguishing between patients in different risk groups [13].

Figure 3. (A) 6 Necroptosis related genes associated with prognosis (P<0.05); (B) The distribution of risk score; (C) Survival time; and (D-E) Dimension reduction analysis in the TCGA cohort.



We drew a KM curve to identify differences in prognosis between low- and high risk groups. Obviously, the prognostic distinctions were evident. The high risk group had a poor prognosis, whereas the low risk group had a favorable prognosis in the TCGA patient cohort (Figure 4A). Furthermore, our study focused on measuring the Area Under the Curve (AUC) with ROC to validate the accuracy of the model prediction. Specifically, this model can relatively predict the OS of patients with OC at 1, 3, and 5 years, achieving AUC values of 0.573, 0.614, and 0.656 on the test set from the TCGA cohort (Figure 4B), showing that this model can accurately predict the 5 year OS of patients with OC to some extent [14].

In addition to the content mentioned above, independent prognostic analysis was needed in assessing the acceptability of the risk score in the prediction of prognosis independent of any other clinical prognostic features, such as age, tumour grade, and stage. Univariate Cox analysis predicted that in the TCGA cohort, age, stage, residual tumour after tumour reduction surgery and risk score were closely related to the OS of patients with OC ($P < 0.05$, Figure 4C). On the other hand, when the interplay among various clinicopathological variables was considered, the multivariate Cox analysis was applied, and a similar conclusion was reached age, residual tumor and risk score were still closely associated with OS ($P < 0.01$, Figure 4D).

Validation of the prognostic risk model

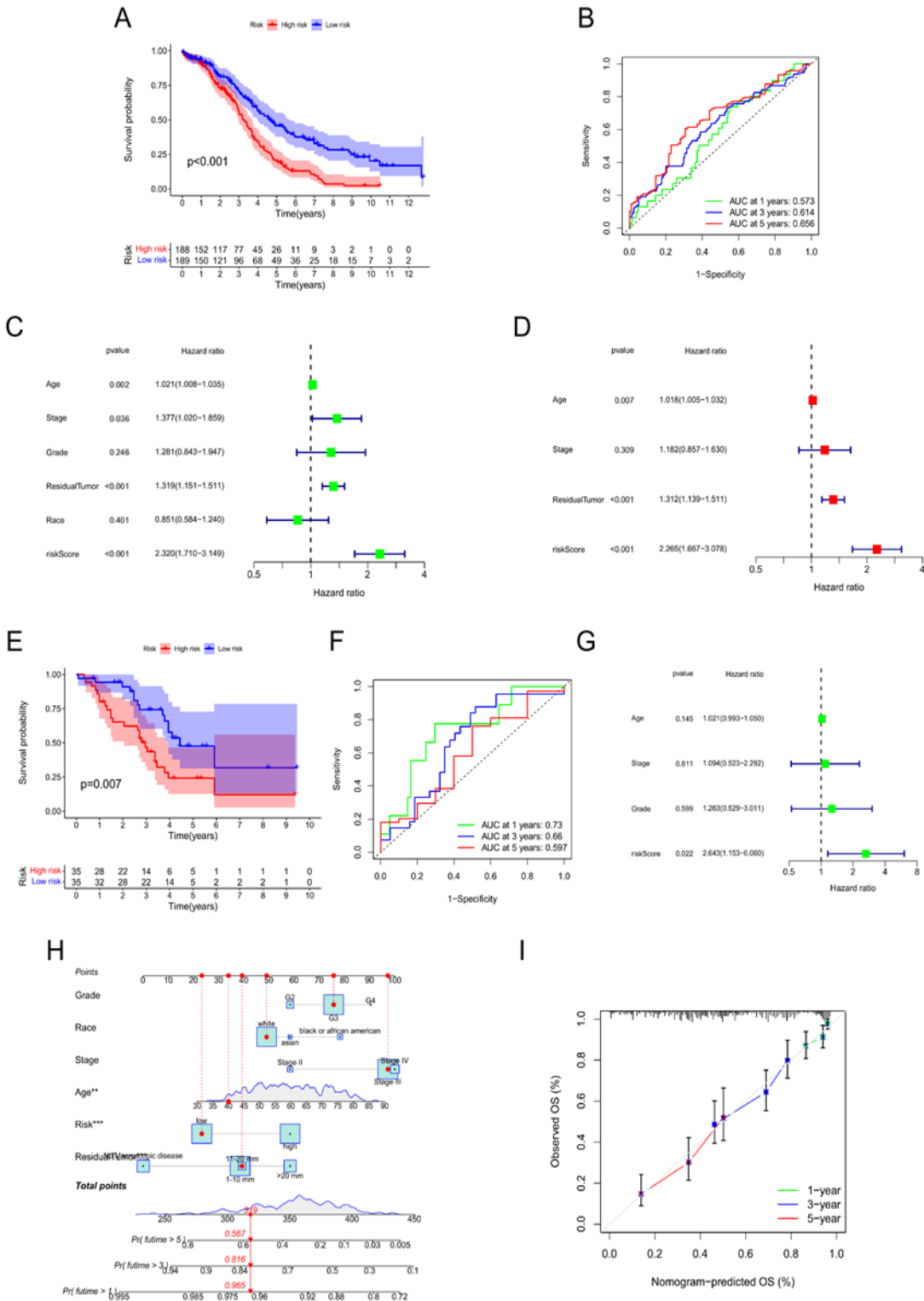
To test the predictive power of gene signature, we tested it using the TCGA cohort as an internal test cohort and validated it on another independent GEO patient cohort. Thus, we extracted genes from the three gene signature model and constructed a multivariate Cox regression model in the GEO database. Likewise, on the basis of the median risk score from the GEO cohort, the OC cases were classified into high- and low-risk groups. Then, we calculated the survival rates of patients according to KM survival in different risk groups. The high-risk group had significantly worse survival outcomes than the low-risk group (Figure 4E). Furthermore, the ROCs of patients with OC from the GEO dataset (GSE19829) reconfirmed the accuracy of our prediction model to some extent, and the AUCs were 0.73, 0.66, and 0.597 (Figure 4F). Finally, in the validation of GSE19829, we found that only the risk score can be validated, which offers prognostic information regarding the survival outcomes of patients with OC according to the univariate Cox analysis, compared with known prognostic clinical factors (Figure 4G).

Construction of a nomogram

Nomogram was constructed based on various prognostic indicators and risk scores to predict 1, 3, and 5 year survival in OC patients, respectively (Figure 4H). The calibration curve (Figure 4I) demonstrated the excellent predictive power of the Nomogram [15].

Figure 4. Verification of the predictive three gene signature. KM curves in the TCGA group (A) and GSE19829 data group (E). The ROC curve over time in the TCGA group (B) and GSE19829 data group (F). Independent prognostic analysis of the risk score in the TCGA group (C-D) and GSE19829 data group (G). The Nomogram for predicting the 1-year, 3-year, and 5-year overall survival rate of OC patients (H). The calibration curve to evaluate the accuracy of the Nomogram model (I).

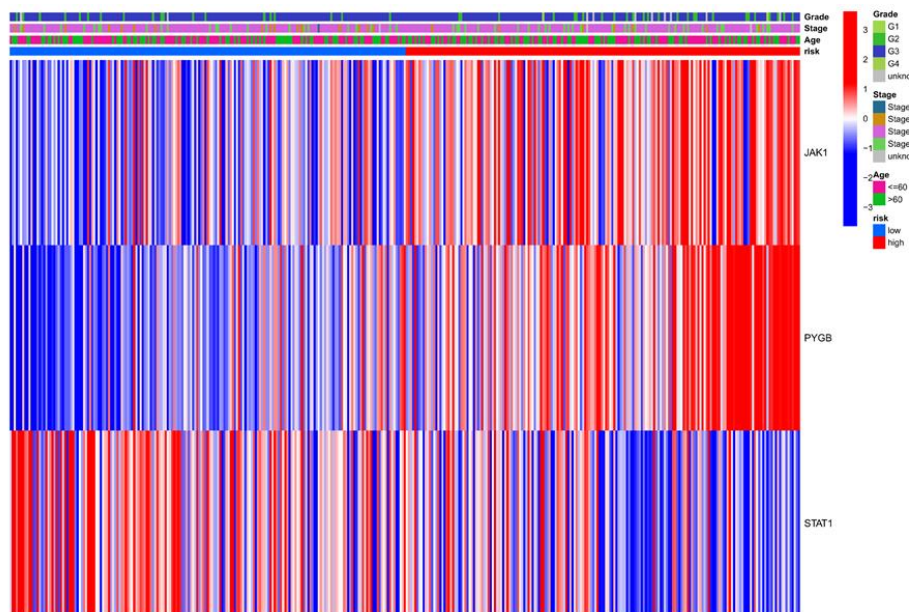
Identification of High-Risk or Low-Risk genes.



Identification of high risk or low risk genes

As shown in the heat map, the OC cases from the TCGA database were grouped into different risk groups. The high expression of each gene involved in model construction was indicated in blue, whereas low expression was given in red. From left to right, the expression of *JAK1* and *PYGB* increased with the risk of patients, whereas *STAT1* expression decreased with increasing risk of patients. These results demonstrated *JAK1* and *PYGB* were high-risk genes and *STAT1* belonged to low risk gene. Unfortunately, no statistically differences in the clinical traits of OC cases (e.g., grade and stage) were found between the low and high risk groups (Figure 5) [16].

Figure 5. The expression of three genes involved in model construction and differences in the clinical traits including grade, stage, and age between the low and high risk groups.



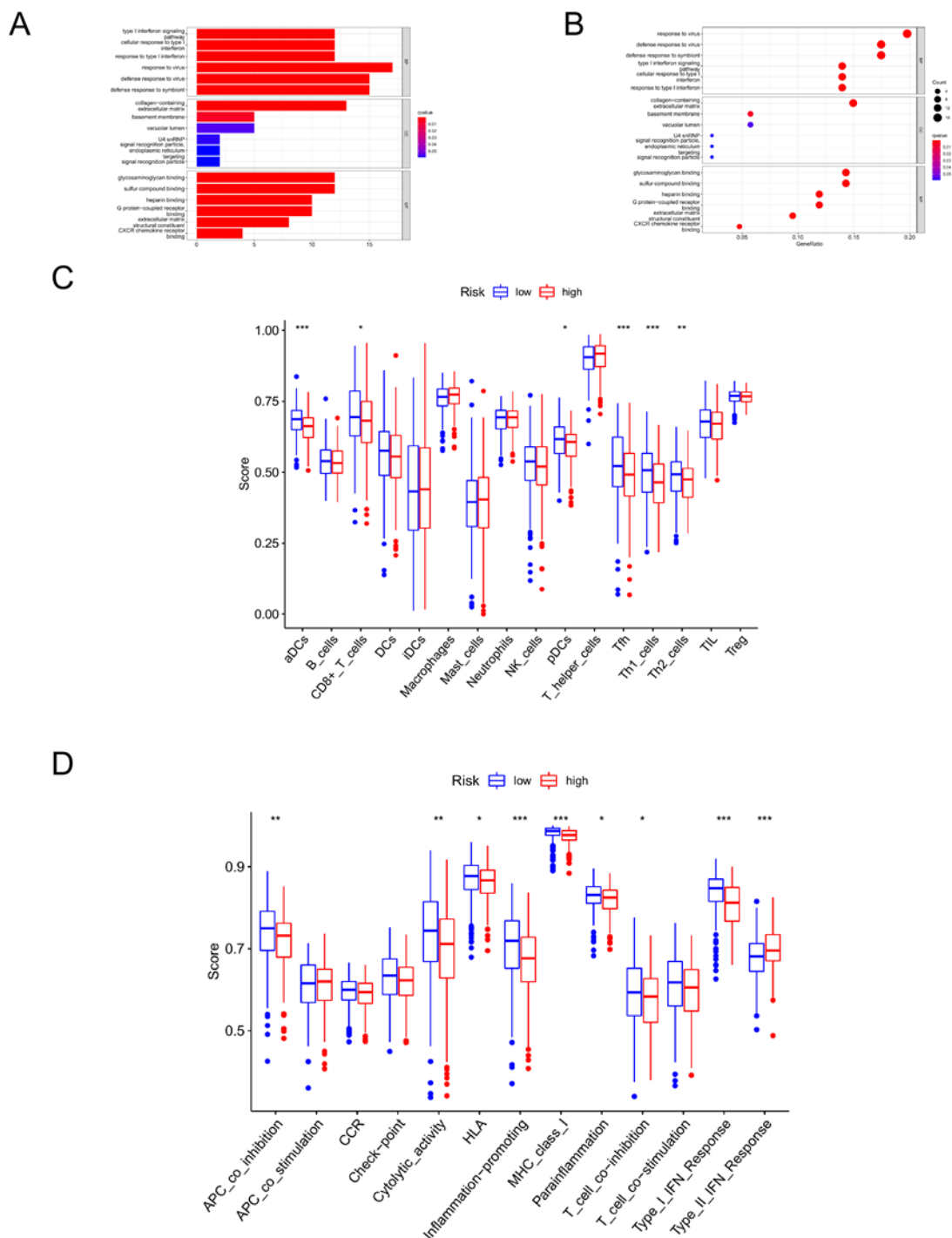
Functional enrichment analysis of DEGs in high and low risk groups

Patients with OC in the TCGA dataset were divided into two risk groups, namely low and high risk groups. Subsequently, when $FDR < 0.05$ and $\log_2FC > 0.585$, we screened 105 significant necroptosis related DEGs between the two groups and performed downstream functional enrichment analysis. As shown in Figure 6A and 6B, Gene Ontology (GO) analysis of the candidate genes revealed strong enrichment of functions associated with type 1 interferon, response to virus, and defence response to symbiont. Only four enriched terms were identified in the subsequent KEGG pathway analyses, including the interactions of viral proteins with cytokines, hepatitis C, influenza A, and chemokine signalling pathway.

Immune related analysis of DEGs in high and low risk groups

Notably, apparent differences in immune cell types or immune functions between different risk groups are shown in Figure 6C and 6D. For example, aDCs, CD8+T cells, Tfh, APC co-inhibition, inflammation promoting, and type-I-IFN response, were upregulated in the low risk groups, whereas type-II-IFN response were significantly up regulated in the high risk groups (** $P < 0.001$; * $P < 0.01$; $P < 0.05$).

Figure 6. (A-B) GO functional enrichment analysis of DEGs. (C) Differences in immune cell types; and (D) Immune functions between low and high risk groups.



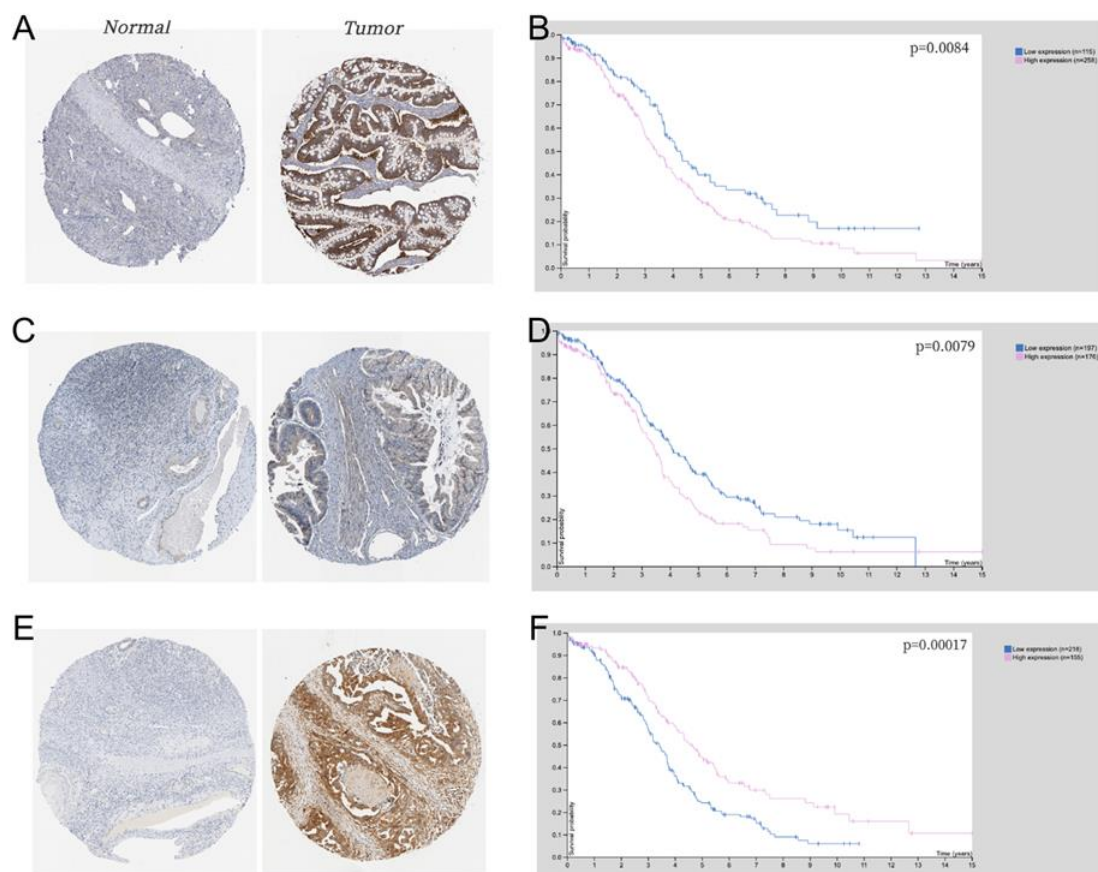
Overexpression of each gene involved in model construction in tumour tissues

As shown in the previous section, *PYGB*, *JAK1*, and *STAT1* played important roles in the construction of our necroptosis model. To further demonstrate the level of *PYGB* in OC, the HPA database was used in confirming the expression of *PYGB*. As shown in Figure 7A, the expression of *PYGB* was enhanced in the OC tissues compared with those in the normal ovarian

tissues. Subsequently, the relationship between *PYGB* expression levels in OC and prognosis was analyzed. Among the 373 OC cases, 258 cases were highly expressed with a 5-year survival rate of 29%, and 115 cases showed low expression with a 5-year survival rate of 40%. These results indicated that a high *PYGB* expression tends to be inversely linked to the prognosis of OC patients (Figure 7B, $P=0.0084$). We successively showed the expression levels of *JAK1* and *STAT1* in normal and tumor tissues. Both genes showed higher expression levels in OC than in normal tissues (Figure 7C and 7E). As for the relationship between *JAK1* and prognosis, patients with OC and high *JAK1* expression had significantly reduced 5-year OS rates relative to patients with low *JAK1* expression (Figure 7D, $P=0.0079$). By contrast, the 5 year survival rates of *STAT1* in the high and low expression groups were 45% and 24%, respectively, indicating that the overexpression of *STAT1* is associated with improved prognosis (Figure 7F, $P=0.00017$). Thus, we speculated that *JAK1*, similar to *PYGB*, is an unsuitable prognostic marker, whereas *STAT1* expression is a favorable biomarker for OC [17].

All these data suggested that each gene involved in model construction plays a crucial role in the occurrence and progress of OC.

Figure 7. Immunohistochemistry of three genes involved in model construction in tumor and normal ovarian tissues: (A) *PYGB*, (C) *JAK1*, and (E) *STAT1*. The KM curve of each gene involved in model construction between the high and low expression groups: (B) *PYGB*, (D) *JAK1*, and (F) *STAT1*.

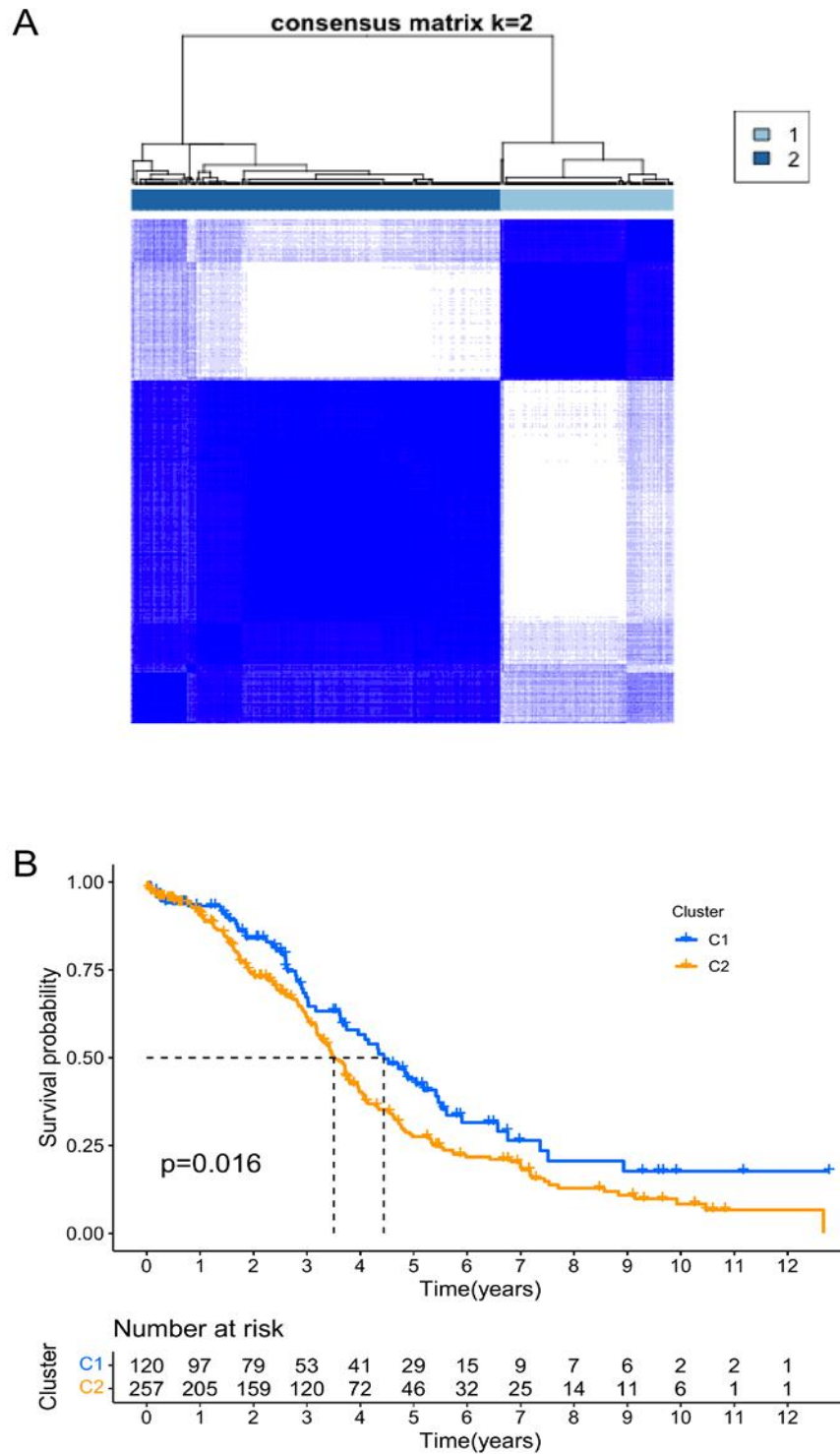


Tumour typing and typing survival analysis

Through consensus clustering analysis, we observed that $k=2$ is the most suitable option for subtyping patients with OC

(Figure 8A). Thus, when clustering stability was considered, patients with OC were separated into two subtypes, namely clusters 1 and 2. The KM curve indicated striking differences ($P < 0.05$) between the two clusters. Specifically, the survival rate of the patients in cluster 1 was better than that of the patients in cluster 2 (Figure 8B) [18].

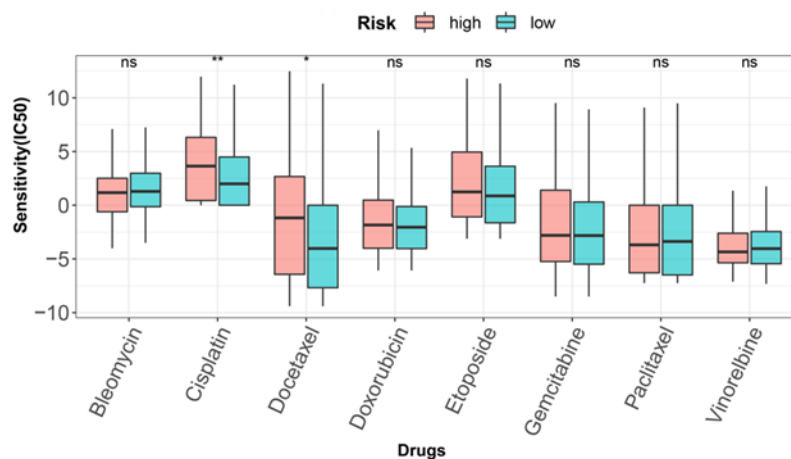
Figure 8. (A) Tumour typing; and (B) The KM curve of OC patients between two clusters.



Drug sensitivity analysis

To screen out potential drugs for the treatment of ovarian cancer, we further analysed and predicted the differences in the sensitivity of different chemotherapy drugs in high and low risk groups (Figure 9). The results showed the half maximal Inhibitory Concentration (IC₅₀) values of cisplatin and docetaxel in the high-risk group were higher than those in the low risk group, suggesting that patients in the low risk group were more sensitive to these drugs. However, no significant differences between different risk groups in the IC₅₀ values of other drugs were found.

Figure 9. IC₅₀ values of eight representative drugs between the two risk groups.



DISCUSSION

In this study, we first identified 120 necroptosis related DEGs in OC and normal ovarian tissues by using different public databases. Then, we constructed a three gene (*JAK1*, *PYGB*, and *STAT1*) risk prediction model through univariate and multivariate regression analysis and verified the model in an internal training cohort and external validation cohort to further evaluate the prognostic value of the necroptosis related DEGs. Subsequently, the OC cases in the TCGA dataset were divided into high- and low-risk groups according to the median of the risk scores. DEGs in the two risk groups were subjected to functional enrichment analysis and immune related analysis [19].

OC, one of the leading causes of death among women, is generally detected at an advanced stage and has a poor prognosis. Thus, further research on specific diagnostic markers, prognostic models, or therapeutic targets, is of imminent importance. In recent years, the relationship between cell death and OC has gained considerable interest, and a series of prognosis models correlated with cell death has been proposed. Some simple examples include an autophagy-related prognostic signature for serous OC. This signature was developed by An, et al. A ferroptosis related gene signature for OC was developed by You, et al. However, the model of necroptosis, one prominent form of programmed cell death, and a potential target for cancer development and therapy, were not involved. Therefore, a necroptosis related risk prediction model is needed to fill the gap.

Our model was composed of three necroptosis related genes, namely, *JAK1*, *PYGB*, and *STAT1*, which were all closely associated with the prognoses of patients with OC. We marked the oncogenes *JAK1* and *PYGB* in red, which are potential

independent risk factors for patients with OC. *STAT1* was marked in blue, which acted as a tumour suppressor gene (Figure 3A).

Metabolic reprogramming, a hallmark of cancer cells, can support cancer cell survival and proliferation. Up regulated glycogen metabolism has recently been recognized as a well-established feature of human cancer cells. Accumulating evidence demonstrates a link between *PYGB*, the essential rate limiting enzyme of glycogen breakdown, and the development and procession of various cancers. For example, *PYGB* is highly up-regulated in various types of cancer including NSCLC, Hepatocellular Carcinoma, etc. The up regulation of *PYGB* was observed in OC and was negatively correlated with OS. These results were consistent with our results in the HPA database. The proliferation of tumour cells and apoptosis can be suppressed and induced, respectively, by inhibiting glycogen phosphatase activity and hindering the degradation of glycogen. *PYGB* knockdown and the resulting inhibition of glycogen utilization can decrease the invasive potential of breast cancer cells. Lee et al., showed that the growth of prostate cancer cells could be suppressed, and apoptosis can be induced by silencing *PYGB* via the NF- κ B/Nrf2 signalling pathway. Similarly, the knockdown of *PYGB* inhibits the growth of human osteosarcoma cell lines and gastric cancer cells. Zhou et al., showed that *PYGB* knockdown significantly suppressed proliferation, invasion, and migration of OC cells via the Wnt/ β -catenin signalling, which might serve as a promising therapeutic target for OC treatment [20].

JAK is a non-transmembrane tyrosine kinase, and *JAK1* is a member of the *JAK* kinase family. Through bioinformatics analysis, we predicted that *JAK1* is a potential oncogene in OC (HR<1). However, *JAK* mostly appears in combination with *STAT* in the form of a signalling pathway to engage in the initiation, development, and progression of cancer. As a classic pathway, *JAK/STAT* signalling comprises three basic parts: tyrosine kinase associated receptor for signal reception, *JAK* tyrosine kinases for transmitting signals, and *STAT* transcription factors for producing functional effects. Janus kinase can respond to various extracellular signals by binding to receptors, such as interferons, interleukins, and growth factors and promotes the autophosphorylation of receptors and the transmission of signals to *STAT*. Activated *STAT* enters the nucleus, binds to target genes, regulates the transcription of downstream genes, and ultimately affects basic cellular functions from differentiation and proliferation to apoptosis. The *JAK* family contains four tyrosine kinases: *JAK1*, *JAK2*, *JAK3*, and tyrosine kinase 2, and the *STAT* family comprises seven members, namely, *STAT1*, *STAT2*, *STAT3*, *STAT4*, *STAT5A*, *STAT5B*, and *STAT6*. Different members in the *JAK* and *STAT* families can be specifically combined to form different signal pathway axes. Thus, some molecule inhibitors have been developed against different *JAK* proteins on this signalling pathway for the treatment of various diseases. As an oncogene, *HOXA10* expression is obviously up-regulated in gastric cancer; enhances cell proliferation, cloning formation, and tumorigenesis abilities; and inhibits cell apoptosis by activating *JAK1/STAT3* signaling berberine suppresses bladder cancer cell proliferation by inhibiting *JAK1/STAT3* signaling by up regulating miR-17-5p33. *SDC-1* suppresses the growth and migration of colorectal carcinoma cells by blocking *JAK1/STAT3* pathways. Similarly, Wen et al. reported that *JAK1* kinase, rather than *JAK2*, is required for the persistent activation of *STAT3* in human OC cells. Targeting the *JAK1/STAT3* pathway effectively can inhibit peritoneal metastasis and the as cite production of OC and may provide a new therapeutic avenue for treating these events in patients with OC.

STAT1 belongs to the *STAT* protein family (see above). As an important transcription factor, *STAT1* has a dual role in different types of cancer. Specifically, *STAT1* can suppress and promote cancer in different aspects, including angiogenesis, cell proliferation, migration, invasion, apoptosis, and immune response, through multilevel interaction and regulation of target genes. As such, as a potential prognostic marker in patients with solid tumours, *STAT1* may be useful in predicting

patient prognosis on the basis of diverse tumour types, acting as a tumour suppressor or oncogene. In accordance with the reported literature, *STAT1* as a tumour suppressor gene is generally involved in the progression of OC. Zhang et al. found that patients with OC display high *STAT1* expression levels, suggesting an improved prognosis in tumor patients. In subgroup analyses, *STAT1* overexpression is associated with longer OS in patients with high grade serous OC. Likewise, a large Brazilian cohort study of patients with OC showed that high *STAT1* expression is significantly and independently corrected with improved prognosis OS and disease free survival. Furthermore, we utilized the HPA database to confirm the expression of *PYGB* in OC and normal ovarian tissues, and our results were basically consistent with these findings.

Novel antitumor therapies that target the PD-1 receptor and its ligands (PD-L1) can reverse cancer-mediated immune evasion. A set of data by Liu, et al., suggested that *STAT1* and PD-L1 are overexpressed in OC and showed a positive correlation between the two, suggesting the feasibility of targeting the PD-1/PD-L1 in patients with OC. Conversely, a recent study confirmed that up-regulated *STAT1* induces EOC cell proliferation, migration, and invasion; whereas its inhibition suppresses the proliferation, migration, and invasion of the EOC cells. The reason for discrepant research findings might be the molecular mechanism of cross talk between the *STAT1* and TGF- β signaling pathways.

Additionally, enrichment analysis showed that our necroptosis related DEGs between different risk groups were mainly involved in type I interferons and the interactions of viral proteins with cytokine and cytokine receptors. The interferon family comprises three distinct types: type I interferons (IFN- α and IFN- β), type II interferons (IFN- γ), and type III interferons (IFN- λ). Type I interferons initiate antiviral immunity. However, they can also repress tumor development by inducing antitumor immune responses. Moreover, they activate the canonical *JAK/STAT* signaling pathway, thereby inducing hundreds of interferon stimulated genes to exert antiviral and immunomodulatory functions. Thus, we speculated that necroptosis modulates immune response in the tumour microenvironment. The subsequent immune analysis demonstrated different levels of decreases in immune cell functions or different levels of infiltration of multiple immune cell types in the high risk subgroup compared with the low risk group, which was indicative of impaired immune function in the high risk subgroup. However, the score of type-II-IFN response was significantly higher in the high risk group than in the low risk group. Unfortunately, the reasons for this difference are unclear and worthy of further study.

As the deadliest gynecological cancer, early treatments of OC are also vitally important. In addition to surgery, platinum based drugs (cisplatin/carboplatin) and taxanes (paclitaxel/docetaxel) are the most common agents of current OC therapy. The drug sensitivity analysis uncovered patients in the high-risk group were more sensitive to cisplatin and docetaxel. Still, there were no significant differences between different risk groups in the IC_{50} values of paclitaxel. Nearly 20% of ovarian cancer patients are resistant to the standard platinum based chemotherapy, making chemoresistance a significant challenge in ovarian cancer therapy. In patients with platinum sensitive recurrent ovarian cancer, the use of anti-angiogenic drugs, Poly (ADP-Ribose) Polymerase (PARP) inhibitors and other molecularly targeted drugs for maintenance therapy after platinum sensitive chemotherapy. While the pRRophetic R package includes 238 drugs, and only eight were selected targeting ovarian cancer. Unfortunately, they do not have Bevacizumab and other PARP inhibitors (such as olaparib, niraparib and rucaparib). The International Federation of Gynecology and Obstetrics (FIGO) and the National Comprehensive Cancer Network (NCCN) guidelines specifically discuss the (BEP) regimen (bleomycin, etoposide, and cisplatin) separately, especially for use in interstitial tumors of the sex cords. However, the efficacy of carboplatin in combination with paclitaxel in ovarian granulosa cell tumors is comparable to that of the BEP regimen and has lower adverse effects, so the NCCN guidelines currently remain to recommend paclitaxel+carboplatin chemotherapy as a first line regimen for the treatment of

interstitial tumors of the sex cords. However, our drug sensitivity analysis showed no significant differences in the IC₅₀ values of bleomycin and etoposide between the high and low risk groups. The same was true for other drugs, including gemcitabine, doxorubicin, and vinorelbine.

Collectively, large amounts of data collected from multiple public databases provide unique opportunities for building prognosis models. Thus, we identified three necroptosis related genes, which are closely related to the OS of OC cases. On the basis of these genes, we developed and validated a risk prediction model independent of several clinicopathologic features of patients with OC. The model may help clinicians and researchers assess the prognosis of patients with OC.

CONCLUSION

However, OC is a complex disorder that is impossible to be fully predicted using a unitary model. In this case, we have to acknowledge that our study has limitations. Most importantly, the precision of the model, although tested using public retrospective data, was not validated with prospective data. Another limitation is the incomplete or inaccurate annotation of clinical information and its relatively short term follow-up time in the TCGA and GEO database. We hope that necroptosis based modelling can be smoothly translated into clinical applications for the improvement of the prognostic accuracy of patients with OC and validated in external cohorts composed of OC cases with rich and accurate clinical information.

REFERENCES

1. Lampert EJ, et al. Combination of PARP inhibitor Olaparib, and PD-L1 inhibitor Durvalumab, in recurrent ovarian cancer: a Proof of Concept Phase II Study. *Clin Cancer Res.* 2020;26:4268-4279.
2. Gentric G, et al. PML regulated mitochondrial metabolism enhances chemo sensitivity in human ovarian cancers. *Cell Metab.* 2019;29:156-173.
3. Konstantinopoulos PA, et al. Single arm phases 1 and 2 trial of niraparib in combination with pembrolizumab in patients with recurrent platinum resistant ovarian carcinoma. *JAMA Oncol.* 2019;5:1141-1149.
4. Babic A, et al. Association between breastfeeding and ovarian cancer risk. *JAMA Oncol.* 2020;6:200421.
5. Del Campo JM, et al. Niraparib maintenance therapy in patients with recurrent ovarian cancer after a partial response to the last platinum based chemotherapy in the ENGOT-OV16/NOVA Trial. *J Clin Oncol.* 2019;37:2968-2973.
6. Massarelli E, et al. Combining immune checkpoint blockade and tumour specific vaccine for patients with incurable human papillomavirus 16 related cancer: A phase 2 clinical trial. *JAMA Oncol.* 2019;5:67-73.
7. Terry KL, et al. A prospective evaluation of early detection biomarkers for ovarian cancer in the European EPIC Cohort. *Clin Cancer Res.* 2016;22:4664-4675.
8. Yokoi A, et al. Integrated extracellular microRNA profiling for ovarian cancer screening. *Nat Commun.* 2018;9:4319.
9. de Vries EM, et al. A novel prognostic model for transplant free survival in primary sclerosing cholangitis. *Gut.* 2018;67:1864-1869.
10. Tran AT, et al. MiR-35 buffers apoptosis thresholds in the *C. elegans* germ line by antagonizing both MAPK and core apoptosis pathways. *Cell Death Differ.* 2019;26:2637-2651.
11. Paludan SR, et al. DNA stimulated cell death: Implications for host defence, inflammatory diseases and cancer. *Nat Rev Immunol.* 2019;19:141-153.

12. Roychowdhury S, et al. Receptor interacting protein 3 protects mice from high fat diet induced liver injury. *Hepatology*. 2016;64:1518-1533.
13. Su Z, et al. Cancer therapy in the necroptosis era. *Cell Death Differ*. 2016;23:748-756.
14. Gong Y, et al. The role of necroptosis in cancer biology and therapy. *Mol Cancer*. 2019;18:100.
15. An Y, et al. Development of a novel autophagy related prognostic signature for serous ovarian cancer. *J Cancer*. 2018;9:4058-4071.
16. Chen X, et al. Analysis of autophagy related signatures identified two distinct subtypes for evaluating the tumour immune microenvironment and predicting prognosis in ovarian cancer. *Front Oncol*. 2021;11:616133.
17. Yu Z, et al. A novel ferroptosis related gene signature is associated with prognosis in patients with ovarian serous cystadenocarcinoma. *Sci Rep*. 2021;11:11486.
18. You Y, et al. Ferroptosis related gene signature promotes ovarian cancer by influencing immune infiltration and invasion. *J Oncol*. 2021;99:15312.
19. Ye Y, et al. A novel defined risk signature of the ferroptosis related genes for predicting the prognosis of ovarian cancer. *Front Mol Biosci*. 2021;8:645845.
20. Hanahan D, et al. Hallmarks of cancer: The next generation. *Cell*. 2011;144:646-674.